

## **High-energy x-ray micro-mapping of materials: engineering applications**

**A white paper. by M. Croft (croft@physics.rutgers.edu), V. Shukla, R. K. Sadangi T. Tsakalacos**

### **Introduction and organization**

The use of synchrotron based high-energy x-ray scattering in materials/engineering programs is relatively new to both the synchrotron and engineering communities in the United States. In Europe such efforts are more advanced with engineering beam lines existent or under construction at ESRF in France, at PETRA III in Germany, and at Diamond in England. The industrial support which these beamline's will provide offers a significant competitive advantage to engineering intensive industries in the EU.

The goals of this white paper are three fold. To make the case to the synchrotron community that creation of beam lines for engineering applications is both called for and important. To make the case to the engineering/industrial community that synchrotron based high-energy x-ray can make a significant contribution to enhancing their research and applications programs. Finally to make the case to funding agencies, like the DOE (both the basic science and applied science divisions), the DOD, the NSF and potentially industries, that scientific infrastructure investment in such facilities are very much in the best interest of science/engineering and of the nation. It should be noted that while the focus here is on engineering applications, these facilities would serve many basic science needs as well.

The specific concentration of this white paper will be on the scientific motivation and the pressing need for high-energy white beam energy dispersive x-ray diffraction (EDXRD) facilities for engineering applications. The sectional organization of this white paper is outlined briefly below.

#### 1.) Heterogeneous system characterization: phase and/or chemical changes.

Since the simplest application of EDXRD is in the rapid identification of component crystalline phases, such phase mapping application will be discussed first. It should be noted that this has not been the principal application used heretofore at NSLS-X17B1. Consequently, examples from the literature/Internet will be used to illustrate the potential of the technique. Under this general category of applications the following sub categories will be mentioned.

- a.) Phase and/or chemical changes with time.
- b.) Inhomogeneous Phase and/or chemical distributions in space
- c.) Inhomogeneous Phase and/or chemical distributions in space and time: future applications

#### 2.) Science of the deformation of materials

This has been the principal engineering materials area of productivity at NSLS X17B1. In the main text of this white paper a somewhat brief description of this research area will be made. However, a more extensive catalog of specific examples of engineering application experiments will be included in the appendix "Appendix I NSLS X17B1 Engineering Applications Results". In addition some

background information on selected engineering problems will be included in the appendix “Appendix II: selected illustrations of engineering applications”.

### 3.) Rapid, high-resolution x-ray physical imaging methods

The area of rapid high-resolution x-ray imaging is important in engineering applications and should be a part of the proposed engineering beam line. While this area is noted here details have been neglected. Bringing in additional expertise in this area for beamline planning is clearly called for.

### 4.) Initial experimental requirements/capabilities of the high-energy scattering engineering/materials science beamline.

This section discusses the dedicated-to/centered-on engineering applications beamline required to have a robust program in this area. The core of this beamline would be a superconducting wiggler providing a smooth, continuous white beam spectrum with energies in the 20-190 keV.

## 1.) Heterogeneous system characterization: phase and/or chemical changes.

### a.) Phase and/or chemical changes with time.

An energy dispersive diffraction spectrum, like its angle dispersive counterpart, can be used as a quantitative signature of the presence of a given crystal structure (phase) or mixture of crystalline phases. Hence, by monitoring such spectra as a function of time, temperature, current drawn from a battery etc., one can track phase transformations or chemical changes as a function of time. Due to the highly penetrating hard x-rays used, and the small well-defined diffraction volume possible, one can follow such phase changes deep inside a large specimen such as a battery, an ultra-high temperature furnace etc. as a function of time, temperature, current drawn, environment, applied load etc. In the example below from the literature, the kinetics involved in the cement hardening chemical reaction is illustrated by the time evolution of the Bragg peaks in the EDXRD spectra.

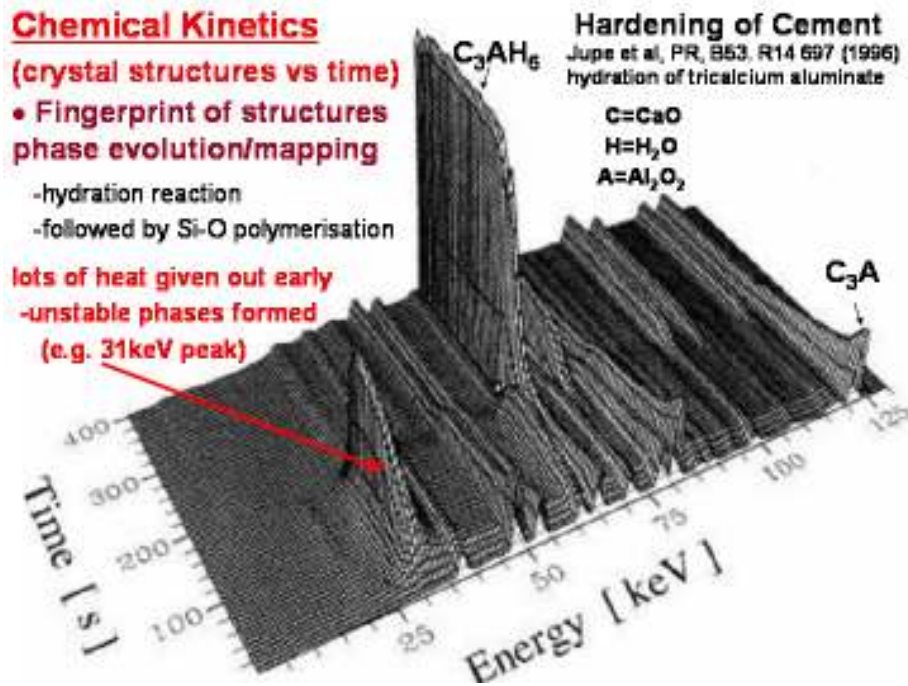


Figure 1. An illustration of the time evolution of the Bragg peaks in an EDXRD spectrum documenting the kinetics of a bulk system chemical reaction e.g. the hardening of cement.

### b.) Inhomogeneous Phase and/or chemical distributions in space

The use of EDXRD spectra to profile separate chemical phases has been used previously by the X17B1 group however it has been more widely exploited in England where the acronym TEDDI is used. Tomographic Energy-Dispersive Diffraction Imaging (TEDDI) involves collecting energy dispersive diffraction spectra as a function

of  $(x,y,z)$  position inside a bulk specimen. The diffraction spectrum at a given point can be decomposed into contributions from separate crystal structures (phase components). The fractions of the differing phase components can then be mapped in 3-D to construct a tomographic image of the distribution of phases. The evolution of the TEDDI data with time, applied stress, current drain etc. can be used to track the spatial evolution, with time, of the chemical reaction or phase change. In the example below a 2-D cross-section diffraction pattern-based mapping of the multiple components in the center of an 80 mm thick concrete block is presented as an illustrated example. Both multiple component mapping and the fact that the cross-section is deep inside a large specimen are important to note. With the increased beam intensity available in the next-generation light sources 3-D mappings would be feasible.

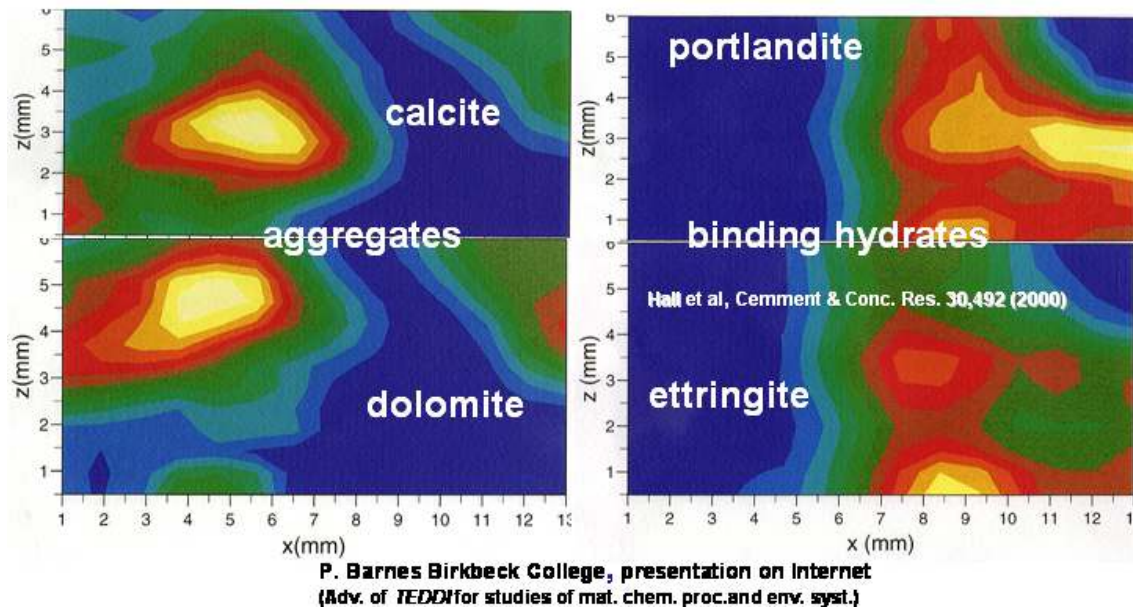


Figure 2. A 2-D crystalline phase mapping of an inhomogeneous system, namely concrete. This  $6 \times 13 \text{ mm}^2$  phase cross-section was taken in the center of an 80 mm thick block of concrete. (Figure taken from the literature and the Internet.)

### c.) Inhomogeneous Phase and/or chemical distributions in space and time: future applications

With illustrations above in mind the extension to both spatial and temporal phase/structure mapping is an obvious one. With the order of magnitude increase in flux available from a wiggler on NSLS-II and a dedicated engineering beam line such space and time dependent mappings would be realizable. Some potential applications of these techniques are noted briefly below.

**Battery applications.** Fundamentally battery applications depend on chemical reactions which proceed in space and time as electronic charge is removed/delivered to different regions in a battery/reaction chamber. While the fundamental laboratory electrochemistry is usually understood detailed structural engineering of new battery

development depend on a myriad of different materials in different layers sealed within a battery containment walls. The nondestructive real time applications of EDXRD-phase-mapping to characterize the functionality/disfunctionality of prototype batteries could provide a valuable tool in the advancement of this field. The pressing relevance of this field from portable electronics, to transportation systems is of course well-known.

**Hydrogen energy transport/delivery applications.** Real world hydrogen storage applications depend on reversible hydrogen absorption or liberation chemical reactions sealed in robust reaction chambers. The ability to use EDXRD to nondestructively map the local chemical changes and to identify material breakdown with cycling could provide important and otherwise unavailable insights into operating prototype systems.

**New/advanced material solid-state chemical synthesis.** Solid-state chemical synthesis of new materials has a long and stellar tradition in both basic and applied science. One need only consider the maelstrom of activity in oxide materials that followed the discovery of high temperature superconductivity to emphasize this point. Many of these materials require trial and error high temperature reactions of constituent oxides in sealed ampoules with multiple constituent ratio trials, high temperature reactions, cool-downs, grinding, intermediate x-ray characterizations, re-pelletizing, resealing, and reannealing steps. EDXRD presents the opportunity for such high temperature phase diagram work to be done rapidly, on a matrix of multiple constituent ratios, continuously as a function of temperature, and under varying gas-flow/vacuum conditions. (Indeed in the NSLS-II plans for an advanced XAS beamline the implementation of a robotically controlled 96 element matrix, with varying constituents and patterned after the standard pharmaceutical industry technology, was specifically address. With high-energy x-rays this method would be even more adaptable to EDXRD.) With EDXRD measurements no intermediate cool downs would be needed in the entire reaction characterization could be fouled in situ. The economy and productivity increase in synthesis of crucial new materials could be tremendous.

**Fuel cell applications.** Currently fuel cell research requires the cooldown dismantling and dissection of fuel cells to identify problems in construction and local chemistry. The highly penetrating character of the radiation used in EDXRD will allow continuous monitoring of the internal regions in an operational fuel cell.

**Characterization of colloidal particles in solutions.** Our group has already performed characterization of particles suspended in colloidal solution and sealed in a glass container. The study of solution based colloidal suspensions and precipitates forming under high temperatures or other reaction conditions would be highly feasible using EDXRD.

**In situ thin film deposition.** The use of EDXRD has already been shown to be possible to characterize in situ growth of polycrystalline thin films. Note that a large touch facility would be required to accommodate this and many of the other proposed applications.

## 2.) Science of the deformation of materials

### Introduction

In addition to yielding a fingerprint of the crystal structure an EDXRD spectrum can be analyzed for the lattice parameters of that structure. The stability of the fixed

angle scattering (with no x-ray optics motion) allows one to determine relative shifts in the lattice parameter of the structure to a relative fractional precision of better than  $0.5 \times 10^{-4}$ . Thus by performing EDXRD measurements on a sample that is translated in the x-y-z directions one can perform 1-D profiles, 2-D maps, or 3-D tomographs of the variation of the lattice parameter within a specimen due to internal strain fields. Such strain field mapping measurements can be used to address a host of fundamental problems in mechanics and materials science. Strain field profiles approaching surfaces or buried interfaces with step sizes down to  $1 \mu\text{m}$  or less will be possible.

It should be noted that this is the engineering applications area in which the NSLS-X17B1-Rutgers group has a wealth of experience. Twelve one page summary examples of X17B1 strain field mapping results are presented in "Appendix I. NSLS-X17B1 Engineering Applications Results" of this white paper. The intent here is to give the engineering and synchrotron specialty readers a robust set of very concrete examples of the EDXRD technique without encumbering the main portion of the text.

There is a large class of unsolved/poorly-understood scientific problems which involve strong nonlinear deformation of polycrystalline materials. Truly successful theoretical modeling of such phenomena, through continuum mechanics, micromechanical and finite element modeling must be grounded upon direct experimental observations on the microscopic length scales upon which the modeling is based. In the past the theories have had to have been constructed on reasonable (but untested) theoretical assumptions due to the absence of such relevant local strain/stress field data. High energy synchrotron radiation-based x-ray diffraction methods have provided proof-of-principle strain/stress field results on this necessary small length scale. Such synchrotron data can serve as a firm foundation upon which to construct solid theories for materials in the strongly nonlinear deformation regime. Indeed, as the work at X17B1 has indicated, entirely new directions for the modeling can originate in the strain mapping results.

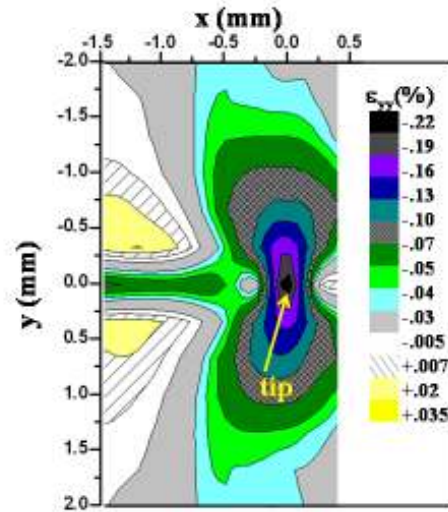
If the engineering beam line recommended in this white paper is constructed the capabilities of NSLS-II will leapfrog the status of strain/stress field mapping from the selected experiments stage, to the stage of providing readily available grounding for theoretical modeling and thence to the stage where new and unexpected observations will dictate new directions in theories. Moreover, with appropriate support a real impact on US engineering infrastructure could be made.

A good example of such experimental driven advances is in the fatigue crack growth problem. Here the stress/strain fields in the vicinity of the crack tip, and the plasticity thereby produced, govern the crack propagation rate. Many years of prodigious modeling efforts in this field have been carried forth virtually without any experimental probe that could directly measure, with sufficient resolution, in the interior of a specimen, the crack tip strain fields upon which the models are based. Quantification and model based descriptions of fatigue crack growth have most certainly had empirical successes, but it has been through the resourceful exploitation of strain/stress measurements remote from the crack tip, along with other indirect and macroscopic measurements.

As an illustrative snapshot of the new type of high spatial resolution synchrotron data now influencing the fatigue crack field, we refer the reader to Figure 3. The figure shows a map of the load-direction strain field component in the vicinity of a fatigue crack tip (in a steel specimen) subjected to a 100 % overload cycle. The large butterfly shaped

compression (extending above and below the crack tip) is caused by the plastic deformation at the overload and is intrinsically involved in the so-called “overload effect” whereby crack growth is retarded subsequent to such an overload.

Figure 3. A high spatial resolution contour plot of the  $\epsilon_{yy}$  strain component near the crack tip of a fatigued steel specimen. These data were taken at X17B1 at NSLS.



As noted above the reader is referred to Appendix I for much more extensive illustrations of engineering problem EDXRD results.

Future applications of the EDXRD technique would involve stress/strain mapping produced by strongly nonlinear stress concentrations. Such concentrations could result from inhomogeneities (like cracks or inclusions) or required component geometrical effects. The study of fatigue crack nucleation, and growth and their interaction with the environment, for example under salt water solution, or other corrosive environments would be a natural component to the research. In all cases both the residual (zero load) and the in situ load induced strain fields would be measured. Stress corrosion cracking would be an important example of real world engineering stress/environment interactions. Of course elevated temperature environments would be part of the studies also.

Many classic and advanced materials are in fact either inhomogeneous mixtures of components or homogeneously organized mixed components. The relative strain response of the separate components in both of these cases could be monitored independently. Classic examples of inhomogeneous mixed materials are of course the two  $\alpha$  and  $\beta$  phases in the aerospace Ti alloys, the competing phases in steels and the Al-matrix/precipitates in advance aluminum alloys. Ceramic coatings on metals, mixed fibrous and homogeneous materials would be examples of intentionally constructed inhomogeneities whose stress dependent response could be studied.

### 3.) Rapid, high-resolution x-ray physical imaging methods

A standard component in the engineering beam lines around the world are a set of rapid and high-resolution x-ray imaging methods. Radiography and element specific enhancement of radiographic images are one example of these techniques. Micro-tomography with both elemental contrast and phase contrast imaging enhancements is most certainly the most prevalent component of these imaging methods. Since many of the elastic measurements discussed above rely on plate like geometries and important additional component would be limited angle tomography to extract detailed, microscopic crack face/tip structure information in cases where total sample rotation is

not feasible. Finally in view of the great expertise in this area already at NSLS a diffraction enhanced imaging component to the imaging should also be included.

#### **4.) Initial experimental requirements/capabilities of the high-energy scattering engineering/materials science beamline.**

A multi-pole superconducting wiggler beamline providing a smooth, continuous white beam spectrum with energies in the 20-190 keV is the core of this facility. The capability of using either a white beam mode or a monochromatic mode should be included as part of this facility. In view of the substantial monetary constraints and intrinsic optics heat load engineering challenges that have become apparent regarding the new beam lines on NSLS-II a second approach to this beamline is also possible. Specifically, the multi-pole wiggler could be installed initially with white-beam-only end-stations/hutches. An x-ray optics enclosure would have to be included for installation of a monochromator a later date. This no-optics option would allow for immediate and cutting edge scientific productivity without the extreme expense and engineering time delays involved in extremely high heat load x-ray optics.

Although this proposal is for an engineering dedicated beamline an interim combination with medical research applications or high-pressure science would not be unreasonable. It is important to note however that an engineering applications first with other applications ancillary is the intent of this proposal.

The central engineering application on this set of touches on this beamline would be EDXRD using the white beam mode. Beam widths/heights down to  $\sim 1 \mu\text{m}$  (or less) will be employed. Typical experiments will involve variable slit sizes depending on the detailed experiment at hand.

A collection of 5-6 hutches will be included. At least three hutches will be able to be run simultaneously (e.g. like X17-A, B, C). The additional hutches will be in sequence so that set up on the last one or two hutches (e.g. like X17-B1, B2, B3) can be being done while experiments are conducted in the front hutch. The hutches should also have large doors for moving equipment in and out. The hutches should be as large as possible, with the last hutches being placed in an appended exterior building with an external loading dock and truck access for heavy equipment.

## Appendix I. NSLS-X17B1 Engineering Applications Results

### 1. Load dependent fatigue crack strain field profiling: NSLS-X17B1 [1]

Motivation: The local strain/stress fields near a crack tip dictate fatigue crack growth. Our groups strain mapping measurements are essentially the first, on the relevant short length scale, upon which valid fatigue crack growth models/theories can be constructed. The “overload effect” is the pronounced retardation in the fatigue crack growth rate produced by single overload cycle. Understanding the overload effect is a crucial element in modeling variable amplitude fatigue crack growth.

Results: This work involved strain profiling in the vicinity of the crack tips, and under variable in situ loading, of steel fatigue specimens with an overload in their fatigue history. The results in the figure are for a maximally retarded post-overload specimen and address the central elements in the “overload effect”. The results evidence a dramatic nonlinear transfer of response from the overload position (behind the tip) at low load, to the crack tip at high load. Since the tip load response is exclusively responsible for crack growth, the observed diversion of the tensile load to the OL-position (rather than the tip) is an important microscopic mechanism underlying the “overload effect”.

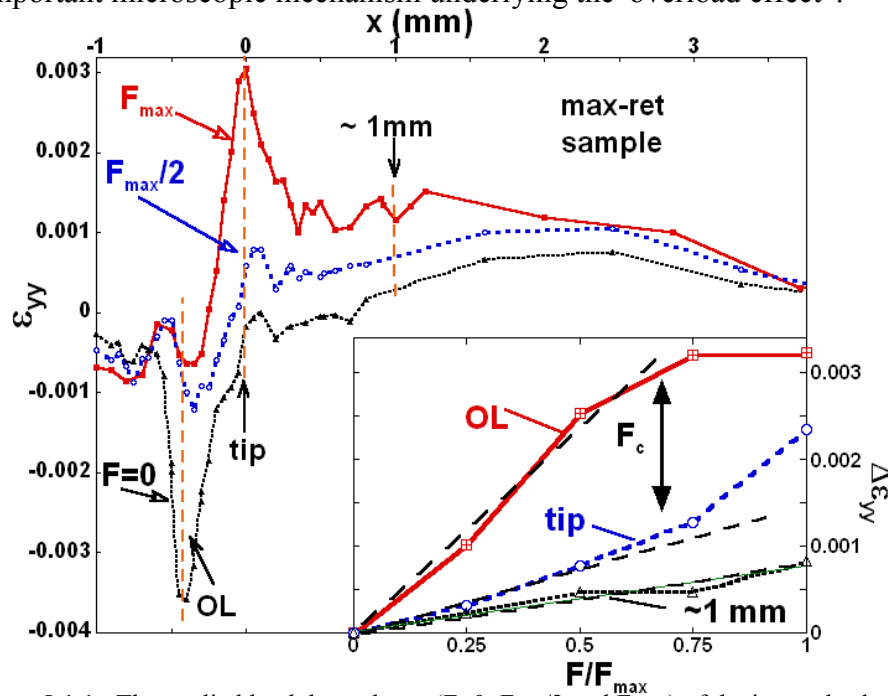


Figure I-1.1. The applied load dependence ( $F=0$ ,  $F_{\max}/2$  and  $F_{\max}$ ) of the in-crack-plane  $\varepsilon_{yy}$ -strain profiles for the post-overload (OL) steel compact tension specimen with maximum crack growth rate retardation (max-ret.).

Inset. A plot of the change in  $\varepsilon_{yy}$ ,  $\Delta\varepsilon_{yy} = \varepsilon_{yy}(F) - \varepsilon_{yy}(F=0)$ , as a function of load at the OL-position, the tip, and a position  $\sim 1$ mm in front of the tip with 5 external loads between  $F=0$  and  $F_{\max}$ . Note the critical threshold load ( $F_c$ ) for transfer of response from the OL-position to the tip.

## 2. Load dependent fatigue crack strain field profiling: NSLS-X17B1 [1]

Motivation: The local strain/stress fields near a crack tip dictate fatigue crack growth. Our groups strain mapping measurements are essentially the first, on the relevant short length scale, upon which valid fatigue crack growth models/theories can be constructed. The “overload effect” is the pronounced retardation in the fatigue crack growth rate produced by single overload cycle, and it’s understanding is a crucial element to modeling fatigue failure.

Results: This work involved strain profiling in the vicinity of the crack tips, and under variable in situ loading, of steel fatigue specimens with an overload (OL) in their fatigue history. The results in Figure 1a &b are for the loads  $F=0$ ,  $F_{max}$ , and  $F_{OL}$  for steel specimens fatigued to various crack lengths beyond the OL. The results of such strain profiles are correlated in Figure 2 with the experimental crack growth curve and a model by Glinka and coworkers (with whom our group works closely). Our microscopic results appear to provide good support for the modeling assumptions.

Figure I-2.1a. The  $\epsilon_{yy}$  residual ( $F=0$ ) strain profiles for a series of steel specimens in the before-OL, after-OL, max-ret. , and 50%-ret. conditions. The position of the OL feature can be seen to move behind the propagating tip (always set at at  $x=0$ ).

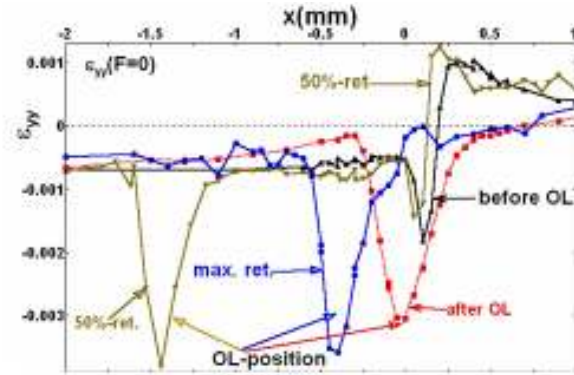


Figure I-2.1b. The  $\epsilon_{yy}$  strain profiles under the maximum fatigue load  $F=F_{max}$  for the before-OL, after-OL, max-ret, and 50%-ret. conditions. The  $\epsilon_{yy}$  strain profile under the OL of  $F=F_{OL}=2F_{max}$  is also included.

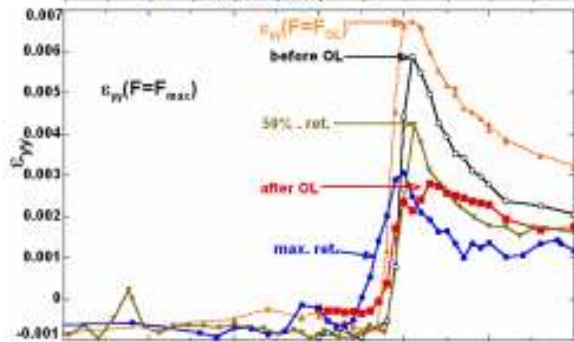
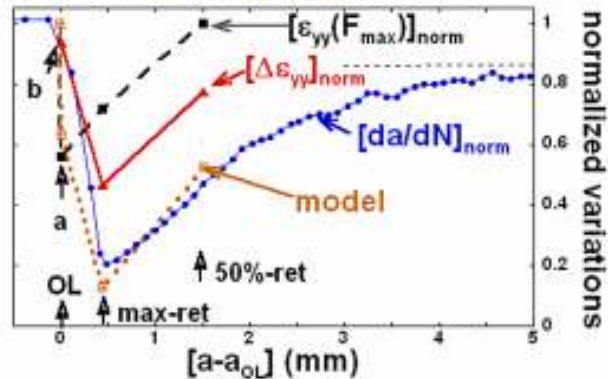


Figure I-2.2. A superposition of the crack growth rate  $da/dN$  and the at-crack-tip values of  $\epsilon_{yy}(F_{max})$ , and of the strain range  $\Delta\epsilon_{yy}$  plotted versus the crack length beyond the OL. All values are normalized to those before the OL. Also plotted is the “model” expression  $\{[\epsilon_{yy}(F_{max})]_{norm}\}^{1-p} \{[\Delta\epsilon_{yy}]_{norm}\}^p$  with  $p=0.83$  and  $\gamma=3$ . [see Noroozi et. al. Int. Jour. of Fat. 27, 1277, (2005) ]



### 3. Residual fatigue crack strain field mapping: NSLS-X17B1 [2]

Motivation: The local strain/stress fields near a crack tip dictate fatigue crack growth. Our groups strain mapping measurements are essentially the first, on the relevant short length scale, upon which valid fatigue crack growth models/theories can be constructed. The “overload effect” is the pronounced retardation in the fatigue crack growth rate produced by single overload cycle, and it’s understanding is a crucial element to such modeling. The 2-D mapping of strain fields around fatigue cracks are required to truly check cross-sections of 3-D modeling.

Results: These results provide detailed 2-D strain field mappings for steel specimens with an overload in their fatigue history. Figure 1 shows the strain fields above and below the crack plane around the crack tip with an OL cycle at the tip. Figure 2 shows a steel specimen in which the fatigue crack has been grown  $\sim 1.5$  mm beyond the OL-position. This map shows the fractured-crack-face region on the left with the unfractured region in front the crack on the right. The dramatic OL-strain-field-scar on the fracture face, arcs weakly across the sample depth. The stronger arc of the crack tip front through the depth of the sample is also clear.

Figure I-3.1. A 2-D cross-section mapping of the  $\varepsilon_{yy}$ -strain field in the x-y plane for a steel specimen with an overload (OL). The  $y=0$  defines the crack plane, the crack propagating is in the x-direction with the tip (at  $x=0$ ).

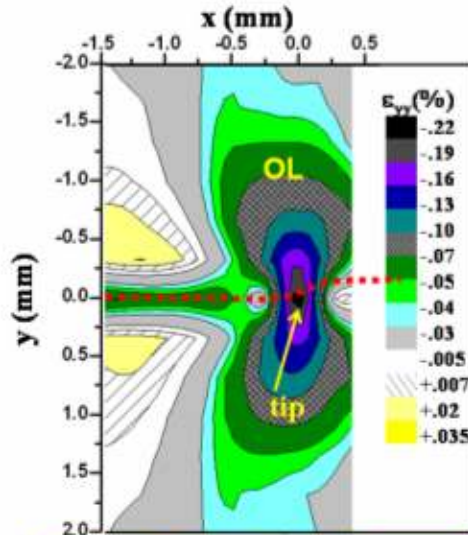
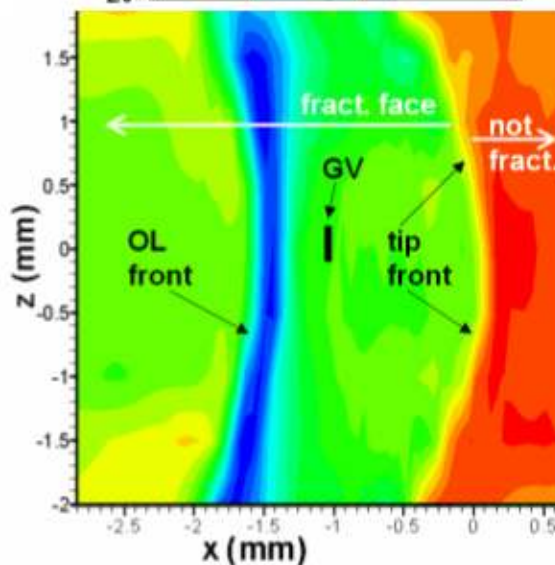


Figure I-3.2. A 2-D cross-section mapping of the  $\varepsilon_{yy}$ -strain field in the crack plane ( $y=0$ ) for the 50%-ret. specimen as a function of the depth  $z$  in the specimen (with  $z=0$  being the specimen center line). The crack tip front separates the fatigue fracture face on the left from the unfractured material on the right. The intense and narrow OL-front is indicated. The footprint of the experimental gauge volume (GV) through the depth ( $z$ ) of the sample is indicated.



#### 4. High-resolution shot peening plastic zone strain profiling: NSLS-X17B1 [3]

**Motivation:** Strain localization under strongly nonlinear deformation is important in diverse scientific fields. Perhaps the widest practical application of this phenomenon the use of shot peening to greatly enhance surface durability/toughness in a multitude of applications, varying from dental picks, to turbojet engine components, to airplane wings, to automotive parts etc. The key shot peening processing parameters are the magnitude and depth of the near surface-compressed plastic zone. EDXRD represents, by far, the best/most-direct technique for probing these key parameters on the required small spatial scale.

**Results:** High strength to weight ratio, corrosion resistance, and high temperature property stability makes Ti-6Al-4V essential for turbojet engine components. Ordinary fatigue, and foreign-object-impact damage induced enhanced fatigue, severely limit the lifetime of such no-fail engine components. Shot peening, is an important life-extending processing technique for such components. The Ti-6Al-4V specimen studied here was shot peened as in jet engine components so the non-destructive detailed characterization of the near surface compressive stress region could be established. The results of this EDXRD study represent essentially the highest spatial resolution (10-20  $\mu\text{m}$ ) and most detailed achieved for such shot peened materials. Moreover, the gauge volume tailoring developed for the different strain components also are unique in this field.

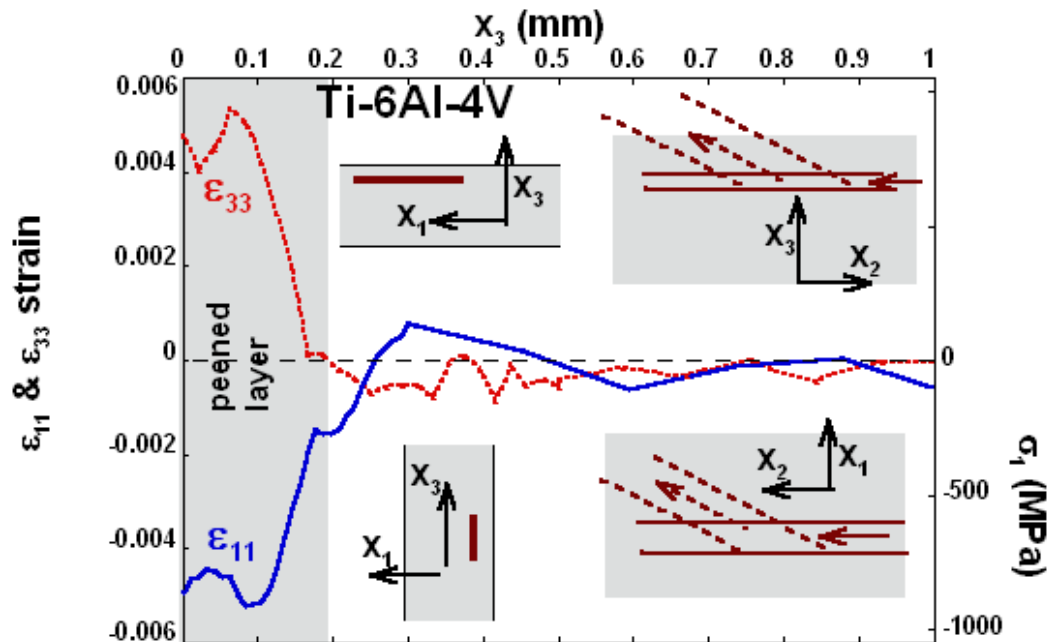


Figure I-4.1. The strain profiles of  $\epsilon_{33}$  and  $\epsilon_{11}$  in the vicinity of the peened surface layer and the underlying bulk material of the Ti-6Al-4V specimen. The insets illustrate the x-ray scattering geometries for the  $\epsilon_{33}$  (top) and  $\epsilon_{11}$  (bottom) measurements. Note the stress scale (lower right) uses  $E=118$  GPa and  $\nu=0.33$  (see text) and  $\sigma_1=175 (10)^3 \epsilon_{11}$  [MPa]. Here  $x_3$  and  $x_1$  are respectively perpendicular and parallel to the peened surface.

## 5. Shot peening plastic zone and deep elastic response strain profiling: NSLS-X17B1 [3]

Motivation: Shot peening is widely used to enhance surface durability/toughness in a multitude of applications. The key shot peening processing parameters are the magnitude and depth of the near surface-compressed plastic zone. EDXRD represents by far the best/most-direct technique for probing these key parameters on the required small spatial scale. Introduction of such a compressed surface region requires accommodating stresses in the interior of processed components. EDXRD also provides an excellent method of probing these deep-interior accommodating stresses.

Results: SAE 1070 spring steel is used as a standard in the shot peening industry. The compressed surface region induces a curvature in such steel plates which has long been used as an empirical standard of the “peening strength”. In this study both the in- and out-of- plane strains, and the derived stress variation in the plastically deformed peened surface region were determined. Moreover, the elastic curvature of the underlying material was precisely characterized as a function of depth through the entire specimen thickness.

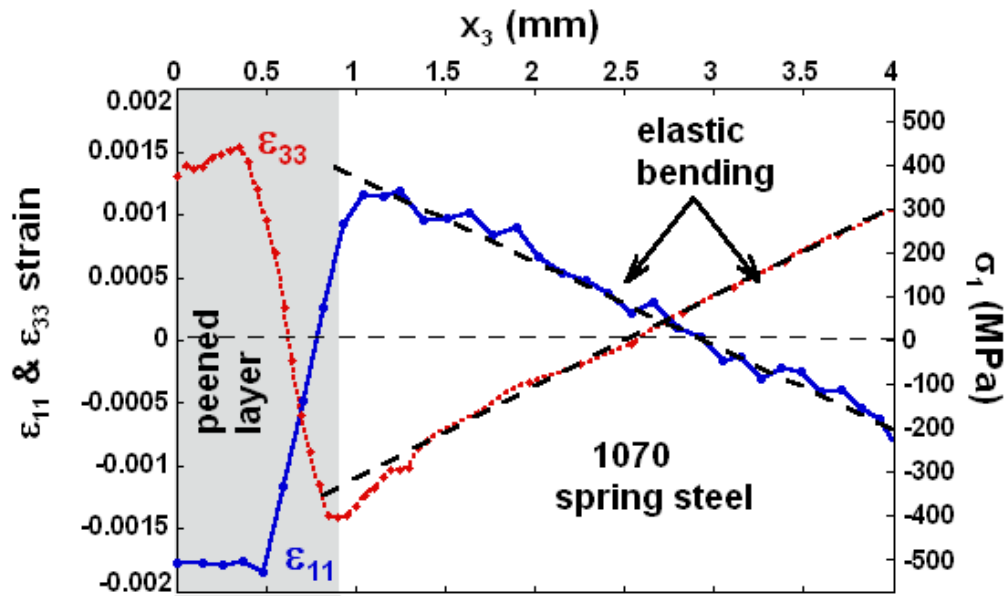


Figure I-5.1 The strain profiles of  $\epsilon_{33}$  and  $\epsilon_{11}$  across the entire thickness of a heavily peened 1070 spring steel specimen. Here  $x_3$  and  $x_1$  are respectively perpendicular and parallel to the peened surface. Note the stress variation on the right and scale corresponds to the  $\epsilon_{11}$  (blue) curve with and  $\sigma_1 = 286 (10)^3 \epsilon_{11}$  [MPa].

## 6. Fatigue crack wake plastic zone strain profiling: NSLS-X17B1 [3]

Motivation: In contrast to the compression induced plastic deformation in shot peening, fatigue crack growth occurs as the result of localized tensile (positive) stresses, concentrated ahead of the crack tip. This leads to plastic deformation, strain localization and eventually fracture. The propagation of the crack tip leaves behind it a deformed plastic wake at the crack faces. The purpose of this study was to characterize the anisotropic strains in this plastic wake region for fatigue crack in a SAE 4140 steel specimen.

Results: The schematic inset in Figure I-6.1 illustrates the fatigue crack with the conventional choices of x-axis parallel to the crack, y-axis perpendicular to the crack and the coordinate origin at the crack tip. The variation of  $\epsilon_{yy}$  ( $\epsilon_{xx}$ ) crossing the crack perpendicularly, along the y direction, (at  $x=-2$  mm behind the tip) are shown. The region of strongly nonlinear plastic flow is reflected by the sharp negative (positive) peak in  $\epsilon_{yy}$  ( $\epsilon_{xx}$ ), labeled 1 (and shaded) in the Figure. This plastic wake region occurs within of  $\pm 0.15$  mm of the center of the crack ( $y=0$ ). The results clearly show that in this near-crack plastic wake region, the strain anomaly is highly anisotropic, with  $\epsilon_{yy}/\epsilon_{xx} \sim -0.7$ . Interestingly this tensile driven plasticity manifests a stress anisotropy opposite to that observed for compressively driven **shot peening cases**.

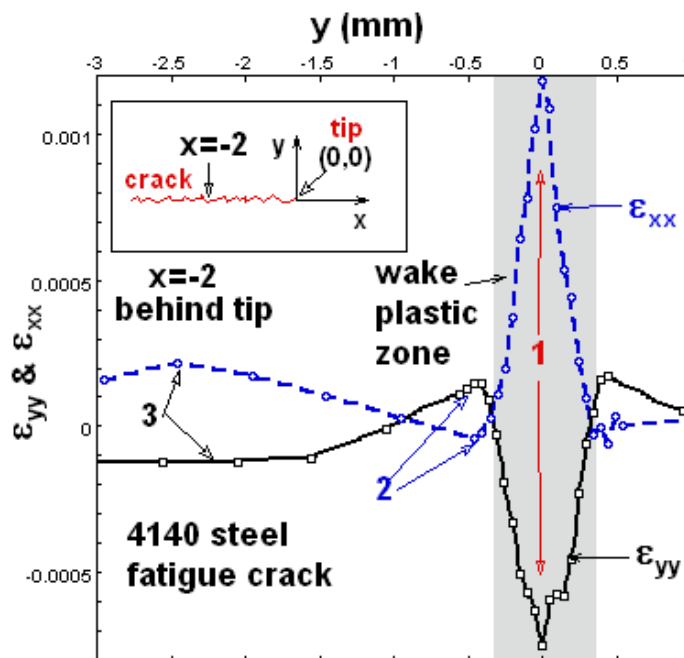


Figure I-6.1. Strain profiles along the y direction (crossing the crack perpendicularly) at a coordinate  $x=-2$  mm (i.e. 2 mm behind the tip) for a fatigued 4140 specimen. The residual  $\epsilon_{yy}$  and  $\epsilon_{xx}$  strain components are shown. Note the sharp anomalies (see label 1 in figure) located at the crack, and the plastic wake zone shaded. The broader background variation (see labels 2 & 3 in figure) farther from the crack are elastic in origin.

## 7. Split sleeve cold working strain profiling: NSLS-X17B1 [4]

Motivation: The stress concentration at rivet/bolt holes makes fatigue failure at such holes an important problem in the aerospace industry. The technique of split sleeve cold working (expansion) of such holes has proved highly effective in forestalling fatigue damage. A detailed understanding of the strains/stresses imposed by this technique are important for optimizing processing parameters. These experiments were intended to prove that EDXRD is a highly effective method for precisely and rapidly profiling the crucial strain fields generated by this technique.

Results: The schematic inset in the Figure illustrates the radial and hoop strains around a split sleeve cold worked (SSCW) hole in an aerospace Ti-alloy specimen. The very large magnitude and deep spatial extent of the compressive hoop stress, induced by the SSCW process, is dramatically detailed in the EDXRD results. The stress concentration which would induce fatigue crack failure is in this hoop direction, hence this substantial SSCW induced compression should lead to greatly extended component lifetimes. This experiment proves that rapid and detailed characterization of optimal SSCW processing conditions by EDXRD is eminently feasible.

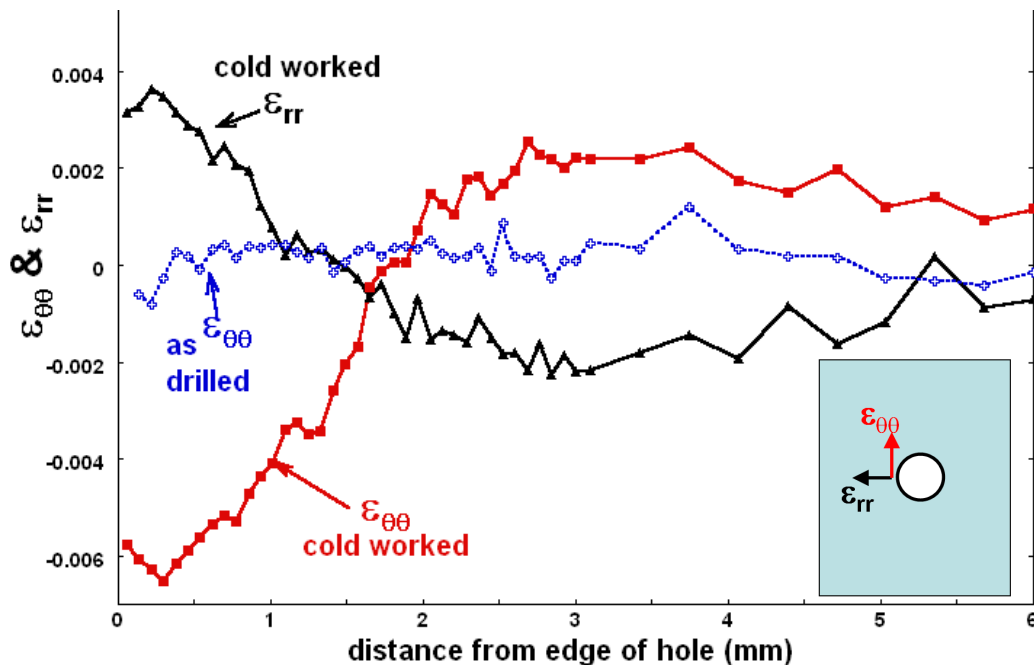


Figure I-7.1. Strain profiles vs. distance from the hole edge of the radial ( $\epsilon_{rr}$ ) and hoop ( $\epsilon_{\theta\theta}$ ) strains around a split sleeve cold worked hole in a Ti-alloy specimen. The as-drilled hole strain profile is shown for comparison. A schematic of the hole and the strain directions is included.

## 8. Laser peening compressive zone and deep elastic response strain profiling: NSLS-X17B1 [4]

Motivation: Surface-initiated fatigue cracking is one of the dominant mechanisms of component failure in engineering applications. Surface toughening processing, like conventional shot peening, is a ubiquitous technique applied to crucial engineering components. Quite recently the technique of laser shot peening (or laser shock processing), LSP, has been developed to provide compressive stresses that extend much deeper below the surface than achievable by shot peening. The LSP deformation mechanism is the shock wave produced by a pulsed laser induced plasma at the surface.

Results: The size of the specimens needed to characterize LSP parameters must be on the order of cm's and hence the deeply penetrating EDXRD method is important for understanding this new processing technique. The high strength to weight ratio, corrosion resistance, and high temperature property stability that make Ti-6Al-4V essential for turbojet engine components also dictated its use in this proof of principle experiment. The x-ray in-sample-path was  $\sim 50$  mm in this experiment. Clearly EDXRD has the deep penetration, high sensitivity, long profile length scale characteristics needed to characterize LSP processed materials.

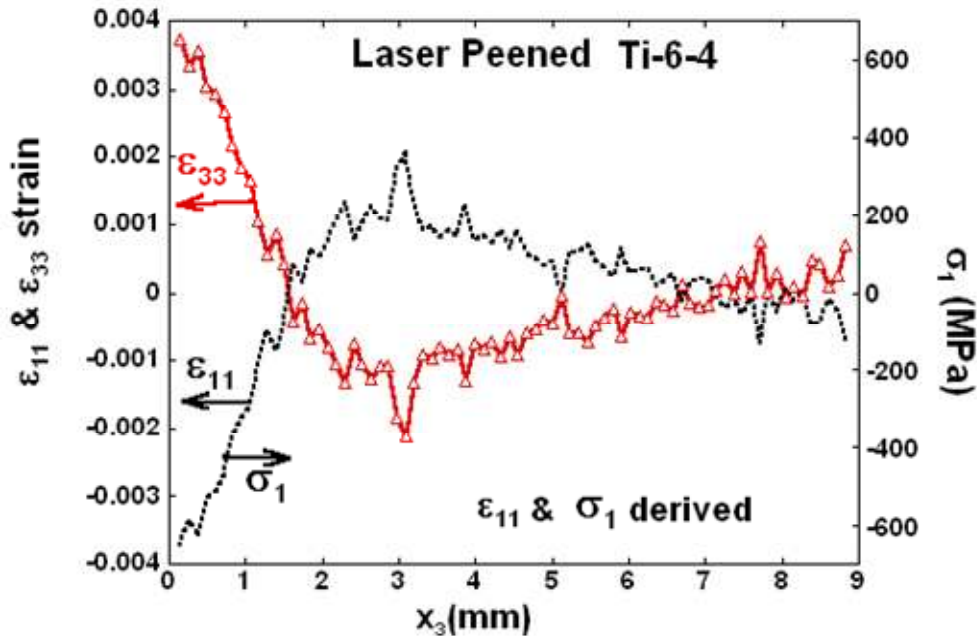


Figure 8.1. The out-of-plane strain profile of  $\epsilon_{33}$  along with the derived  $\epsilon_{11}$  strain and in-plane stress  $\sigma_1$ , for a LSP Ti-6Al-4V aerospace alloy specimen. A biaxial stress state has been assumed here and other work by our group support this assumption. It should be noted that the shot peening process would give a compressive region more than an order of magnitude smaller in depth.

## 9. Weldment residual stress determination; a comparison of IIT and EDXRD techniques: NSLS-X17B1 [5]

Motivation: Residual stresses at weld joints are both ubiquitous and crucial in determining the structural integrity and life expectancy of the weldment. This study profiles the residual stresses produced by a new welding technique, friction stir welding, applied to an advanced fine grained steel API X80. A comparison of the strain profiles obtained from instrumented indentation technique (IIT) and EDXRD technique is made. The in-house IIT measurement is performed on an exposed weldment cross-section. The synchrotron based EDXRD measurement probes a region in the interior of the specimen. Such cross technique comparisons are important in establishing/calibrating such crucial residual stress measurements.

Results: The strain profiles measured by IIT and EDXRD correlate well across the weldment. Here the surface sensitivity of the former and the bulk sensitivity of the latter should be noted. Four microstructural regions can be identified traversing the weldment. In particular the presence of a large compressive stress ( $\sim 300$  MPa) in the Hard Zone of the weldment should be noted. The EDXRD method could in principle be use to map the depth variation of the residual stresses in the internal portions of the weldment.

Figure I-9.1. A photograph of the steel stir weld with four distinct microstructural regions identified.

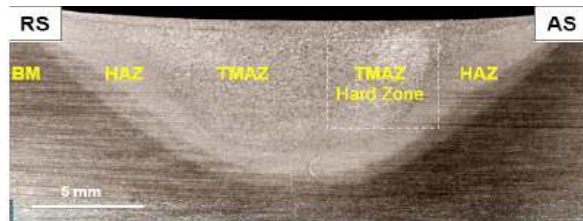
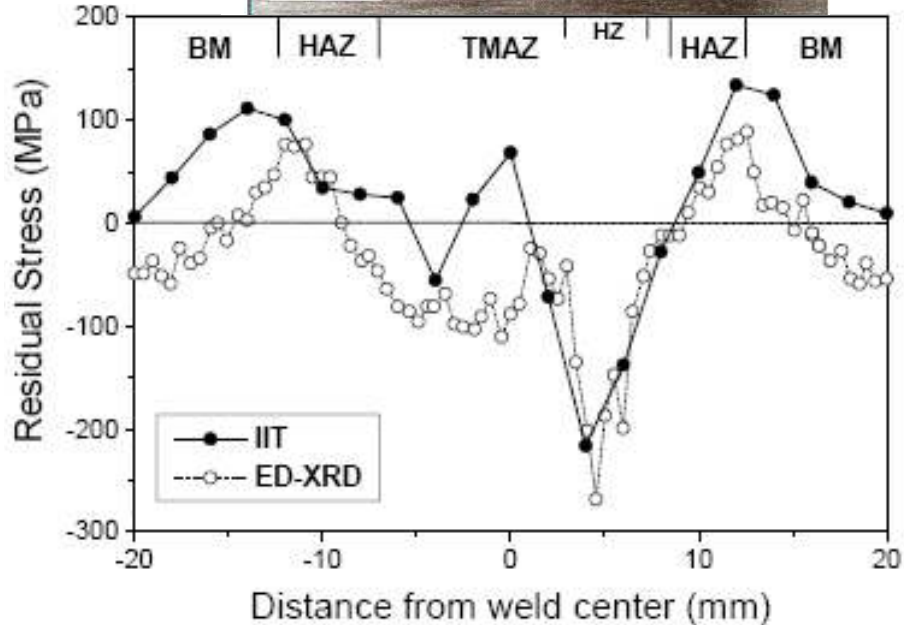


Figure I-9.2. A comparison of the residual stress traversing a steel stir weld by the IIT and EDXRD methods. Note the large compressive stress ( $\sim 300$  MPa) in the Hard Zone region.



## 10. Phase profiling, ceramic coating on metals: NSLS-X17B1 [6]

Motivation: Ceramic coatings on metallic components have achieved substantial success in several areas: in thermal barrier coatings (to support large temperature gradients) as in jet engine components; in wear resistant coatings, as in moving machine components; and in chemical barrier coatings, as in sealing metal surfaces against corrosive salt solutions. One method of applying such coatings is by a plasma spray process. The hot plasma spray process produces a highly non-equilibrium coating which can be dramatically different than the constituents of the powders fed into the plasma. The nondestructive characterization, as function of depth through several hundred microns of the coating, is well-suited to high energy synchrotron x-ray diffraction measurements and is almost inaccessible otherwise.

Results: The figure below illustrates selected diffraction spectra in a phase profiling study of plasma sprayed alumina on Ti specimen. The spectra displacements along the depth ( $x_3$ ) are not linear in position because of the thinness of the  $\sim 200 \mu\text{m}$  coating compared to the thick Ti substrate. The metastable spinel  $\gamma\text{-Al}_2\text{O}_3$  structure of the coating and the very fine ( $\sim 10 \mu\text{m}$ ) resolution depth profiling in the coating should be noted. (Note: the variations in the intensities of the Bragg lines involve x-ray path length absorption effects.) The presence of a very narrow bond coat region and the much larger step sizes in profiling the thick Ti substrate should also be noted.

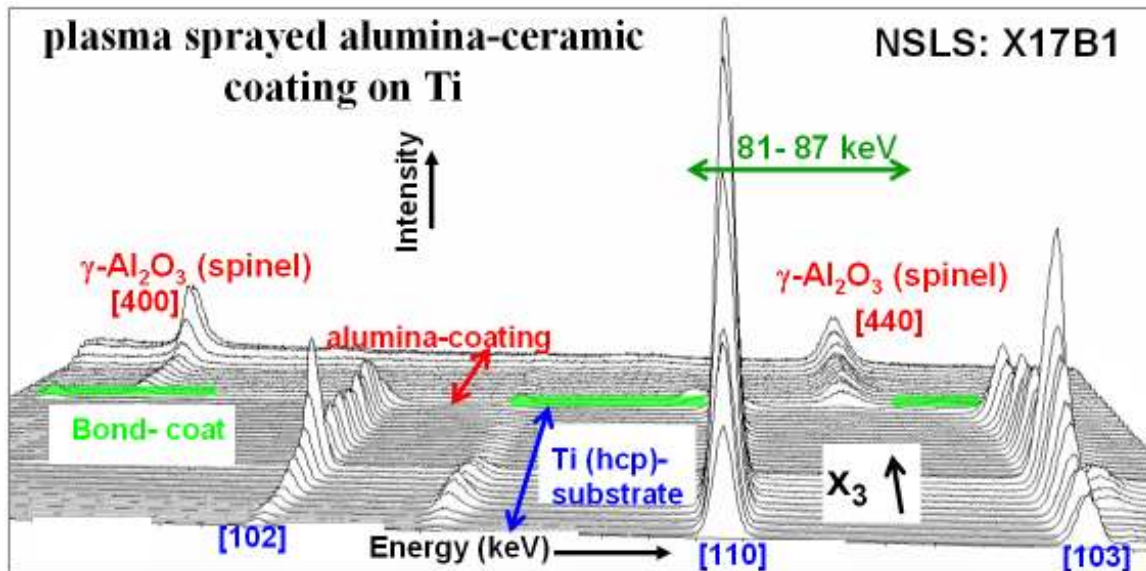


Figure I-10.1. A comparison of the residual stress traversing a steel stir weld by the IIT and EDXRD methods. Note the large compressive stress ( $\sim 300 \text{ MPa}$ ) in the Hard Zone region.

## 11. In situ 4point bending measurement of elastic-plastic behavior: NSLS-X17B1 [6]

Motivation: Ceramic coatings on metallic components have achieved substantial success in several areas: in thermal barrier coatings (to support large temperature gradients) as in jet engine components; in wear resistant coatings, as in rotating machine components; and in chemical barrier coatings, as in sealing metal surfaces against corrosive salt solutions. Bending tests are often used as a lab-floor test for the adherence of such coatings. An in situ 4-point bending apparatus has been developed which allows microscopic EDXRD strain profiling of under bending load. In this experiment the increasing bending moment load was applied to study the increasing elastic/plastic bending response. This is a classic textbook mechanics calculation problem, which is used here to validate the EDXRD in situ load system. Interestingly however, to the experimenters knowledge, no such detailed microscopic investigation of this classic problem has been possible here-to-for.

Results: The figure below shows the in-plane  $\varepsilon_{11}$  strain profiles vs. depth ( $x_3$ ) for 1.6 mm thick Ti plate subjected to varying bending moments ( $M$ ). The classic elastic problem features are abundantly clear: a linear elastic  $\varepsilon_{11}$  strain variation with  $x_3$ ; a central a null plane; and increasing strain slope with increasing  $M$ . Compressive and tensile plastic deformation can be seen to move into the specimen from the edges with still larger  $M$  values. Finally upon releasing the external  $M$ -load the residual stresses in the plastic deformation region and causes a residual elastic curvature of the specimen. Although devised as a test case, such microscopic measurements suggests a number of controlled plasticity investigations.

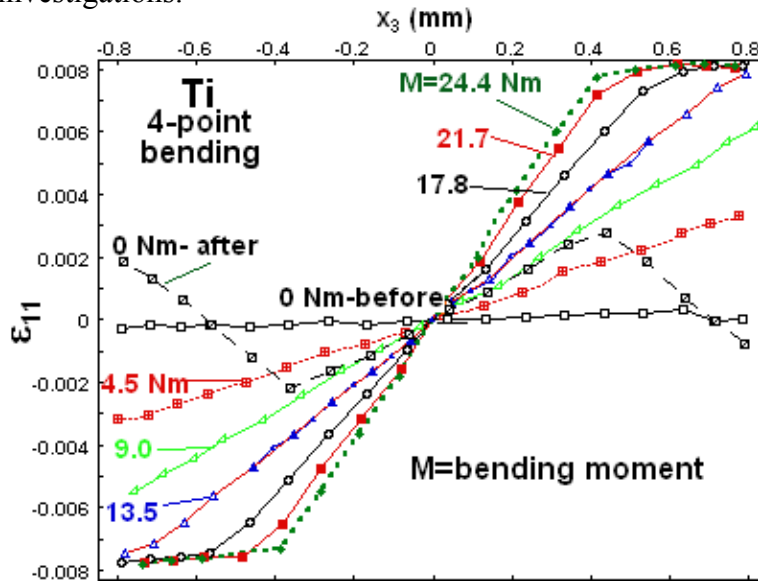


Figure I-11.1. In situ 4 point elasto-plastic bending strain profiles for a Ti specimen.

## 12. Ceramic coating on metals, strain profiling under load: NSLS-X17B1 [6]

Motivation: Ceramic coatings on metallic components have achieved substantial success in several areas: in thermal barrier coatings (to support large temperature gradients) as in jet engine components; in wear resistant coatings, as in moving machine components; and in chemical barrier coatings, as in sealing metal surfaces against corrosive salt solutions. The mechanical properties of the coating-substrate system are of course crucial to the stability of these composite materials. In this experiment the strain response of a plasma sprayed alumina coating on Ti specimen was investigated. This constitutes a first try for the X17B1 in situ bending strain profile method applied to a coated specimen.

Results: The schematic below shows the geometry of the Ti-substrate/alumina-coating specimen in the as-prepared and under 4-point-bending cases. The contour figures plot the scattered intensities versus energy across the specimen thickness. The energy range selected shows both hcp-Ti-substrate and spinel-alumina-coating Bragg lines. The curvature of the Ti line under bending clearly shows the compressive and tensile response. Although the coating response is not discernable in this figure the coating bending response has also been observed.

Figure I- 12.1. (top) A schematic of the Ti/alumina specimen. (bottom) A schematic of this specimen subjected to in situ 4 point bending.

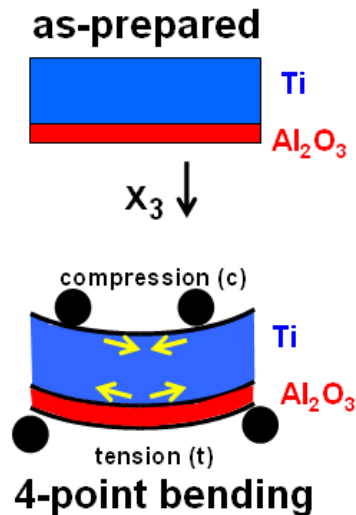
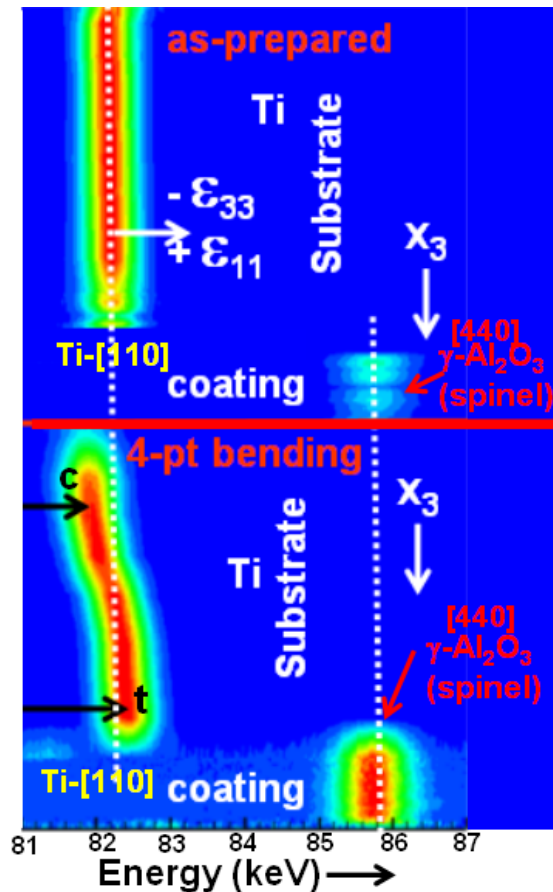


Figure I-12.2. A contour plot, as a function of depth ( $x_3$ ), of the Bragg line diffraction for the alumina/Ti coated specimen. Top panel: the as prepared case. Bottom panel: the specimen under bending with the compressive (c) and tensile (t) deviation of the Ti Bragg line clearly discernable on this coarse scale. Note that the 81 to 87 keV region was indicated in 10. above.



## Appendix I References

[1] Int. Jour. of Fat. 29, 1726-1736 (2007)

M. Croft<sup>1, 2</sup>, N. Jisrawi<sup>3,4</sup>, Z. Zhong<sup>2</sup>, R. Holtz<sup>5</sup>, K. Sadananda<sup>6</sup>, J. Skaritka<sup>2</sup>, and T. Tsakalacos<sup>3</sup>  
<sup>1</sup>Rutgers-Physics, <sup>2</sup>NSLS, <sup>3</sup>Rutgers-Engineering, <sup>4</sup>Sharjah, <sup>5</sup>NRL, <sup>6</sup>TDA Inc.

[2] 16<sup>th</sup> Int. Offshore & Polar Eng. Conf., vol. IV, 57(2006) & work in progress

T. Tsakalacos<sup>3</sup>, M. Croft<sup>1, 2</sup>, N. Jisrawi<sup>3,4</sup>, R. Holtz<sup>5</sup>, Z. Zhong<sup>2</sup>, V. Shukla<sup>3</sup>, R. K. Sadangi<sup>3</sup>,  
& K. Sadananda<sup>6</sup> <sup>1</sup>Rutgers-Physics, <sup>2</sup>NSLS, <sup>3</sup>Rutgers-Engineering, <sup>4</sup>Sharjah, <sup>5</sup>NRL, <sup>6</sup>TDA Inc.

[3] J. Eng. Mat. & Tech. April (2008)

M. Croft<sup>1,2</sup>, N. Jisrawi<sup>3,4</sup>, Z. Zhong<sup>2</sup>, K. Horvath<sup>1</sup>, R. Holtz<sup>5</sup>, M. Shepard<sup>6</sup>, M. Lakshmipathy<sup>7</sup>,  
K. Sadananda<sup>8</sup>, J. Skaritka<sup>2</sup>, V. Shukla<sup>3</sup>, R. K. Sadangi<sup>3</sup> and T. Tsakalacos<sup>3</sup>. <sup>1</sup>Rutgers-Phys.,  
<sup>2</sup>NSLS, <sup>3</sup>Rutgers-Eng., <sup>4</sup>Sharjah, <sup>5</sup>NRL, <sup>6</sup>AF Res Lab WPAFB, <sup>7</sup>Zygo Corp, <sup>8</sup>TDA Inc.

[4] Proof of principle experiment:

M. Croft<sup>1, 2</sup>, N. Jisrawi<sup>3,4</sup>, Z. Zhong<sup>2</sup>, V. Shukla<sup>3</sup>, R. K. Sadangi<sup>3</sup> and T. Tsakalacos<sup>3</sup>. <sup>1</sup>Rutgers-Phys., <sup>2</sup>NSLS, <sup>3</sup>Rutgers-Eng., <sup>4</sup>Sharjah,

[5] ISOPE, 73-76, 2006: D. Kwon, J-S. Lee, J-H. Han, K-H. Kim, R. Ayer, H. Jin and J. Koo;  
Exxon Res. and Eng. : EDXRD performed that X17B1 by T. Tsakalacos<sup>1,2</sup>, Z. Zhong<sup>2</sup> & M.  
Croft<sup>2,3</sup>. <sup>1</sup>Rutgers-Eng., <sup>2</sup>NSLS, <sup>3</sup>Rutgers-Phys.

[6] X17B1 work in progress.

## **Appendix II: selected illustrations of engineering areas where EDXRD could make substantial contributions.**

### **Residual stress engineering and coating induced duty life enhancements**

Fatigue crack failure is accelerated by the presence of tensile residual stresses in engineering components and by the concentration of tensile duty cycle loads. Processing techniques that induce compressional stresses in regions of vulnerability to fatigue cracking can increase the life of such components. The empirical imposition of compressive residual stresses has a long history. Over the years a great deal of effort has gone into specifically engineering processing techniques that will controllably introduce compressive stresses in critical regions to extend component lifetimes.

Ti-alloy compressor fan blades (and other turbojet complements) offer a good example of where such beneficial compressive stress processing has been used and is being expanded. Shot peening has been used for some time in processing such jet engine components. More recently laser shot peening (or laser shock processing) has also become a production line technique choice for these components. Yet another such technique is that of low plasticity burnishing which is now under investigation for this application. It should be noted that outstanding experimental results on both shot peened and laser shot peened materials, performed at NSLS-X17B1, are presented in Appendix I of this white paper.

Another crucial and hostile/demanding environment component in a turbojet engine is the turbine fan blades. These blades must have very high strength at very high temperatures. Some details regarding the use of ceramic thermal barrier coatings in preserving the lower temperature strength of these Ni-super alloy blades is noted below. Here it should be noted that outstanding initial experimental results for similar ceramic coatings on Ti (designed for wear resistance), performed at NSLS-X17B1, are presented in Appendix I of this white paper.

Another area for potential fatigue crack failure is near rivet or bolt holes where tensile loading can create large enhancements of the stress intensity and fatigue cracking. Split sleeve cold working of such holes has proved to be a good method of preventing fatigue cracking around such holes. It should be noted that outstanding experimental results on the residual compressive strains induced by split sleeve cold working, performed at NSLS-X17B1, are presented in Appendix I of this white paper.

Some more details on both the engineering challenges in turbojet components and in split sleeve cold working of holes are presented below.

### Turbo jet engine components

Advanced turbo jet engines for aerospace applications and for energy generation (specifically peak-load generation capacity boosters) require high strength to weight materials operating extremely hostile high temperature and high velocity particle impact environments. Figure II-1 shows a schematic of a turbo jet engine's components.

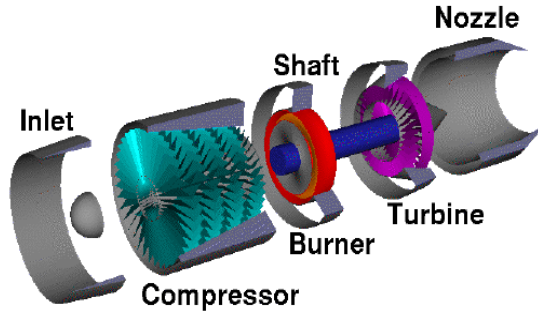
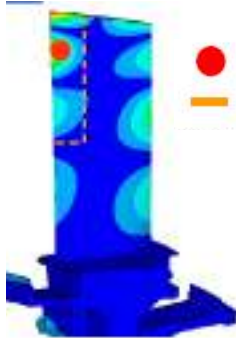


Figure II-1. A schematic of the internal of components of a turbo jet engine such as used in propulsion and energy generation applications. (Internet)

**Turbo jet engines compressor fan blades.** Ti alloy's (such as Ti-6-4) are common in the components of such engines, as for a specific example, in the compressor fan blades (see Figure II-1). Such fan blades undergo substantial fatiguing stresses (see Figure II-2a for example.) Note: 1.) that the front edge of the blade can undergo a particularly high oscillatory fatiguing stress; 2.) that foreign object damage on the sharp front edge is potentially very detrimental to component life; and 3.) that toughening of the front blade surface would therefore be beneficial. In Figure II-2b a test specimen with a notch, to simulate foreign object impact (FOI) damage is seen to provide a stress concentration which nucleates a fatigue crack.



● Peak Vibratory Stress Location  
— Edge of Treatment Zone / Tensile Residuals

Figure II-2a. A simulation of one of the vibrational modes of a Ti-6-4 turbojet compressor blade illustrating the high risk regions for fatigue cracking and FOI. Note that a region for processing induced compressive stresses, to combat fatigue cracking, has been identified. (Proceedings of the 2007 Residual Stress Summit.)

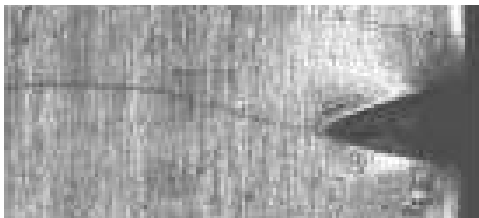


Figure II-2b. A picture of a Ti-6-4 test specimen simulating a fatigue crack initiated at a notch. This test specimen simulates the potential effect of foreign object impact (FOI) on the leading edge of a turbojet compressor blade. (Proceedings of the 2007 Residual Stress Summit.)

In addition to the susceptibility to damage/fatigue at the leading edge other portions of a turbojet compressor blade are susceptible to fatigue cracking. In Figure II-2c a fatigue crack near the base of a compressor blade is shown. Compressive residual

stress processing of such joining sections, subject to stress concentrations, would also be beneficial.

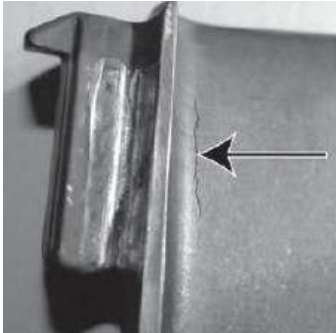


Figure II-2c. A fatigue crack in a Ti-6-4 turbojet compressor blade near the base. (Intenet)

### Turbo jet engines turbine blade.

The turbine blades and a turbojet engine require extreme strength and an ultrahigh temperature environment. The blade itself is typically Ni-super alloy with combinations of complex cooling holes/channels and ceramic thermal barrier coatings (to support a large temperature gradient)

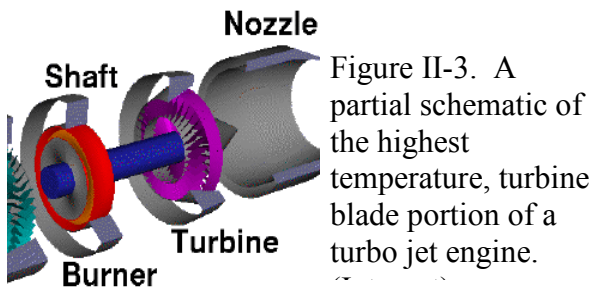


Figure II-3. A partial schematic of the highest temperature, turbine blade portion of a turbo jet engine.



Figure II-4d. A photograph of a turbine blade. Note the complex hole cooling patterning emphasizing the need for engineering intensive design to maintain strength in an ultrahigh temperature environment. Proceedings of the 2007 Residual Stress Summit.)

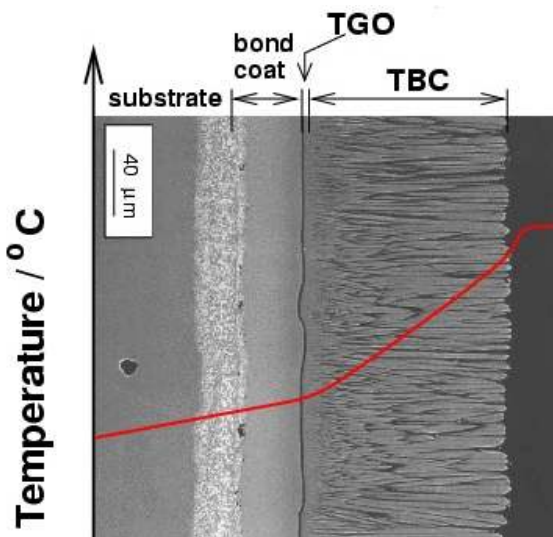


Figure II-4c. An SEM image of a thermal barrier coating (with associated bonding layers) on a Ni-super ally turbine blade substrate. A temperature profile is included to show the temperature gradient supported by the coating to preserve structural strength of the underlying blade. (<http://www.msm.cam.ac.uk/phase-trans/2003/Superalloys/coatings/index.>)

### Hole stress concentrations and split sleeve cold working.

The stress concentration which occurs near a hole under tensile loading and the resulting potential for fatigue cracking are well known and are illustrated schematically in figure II-5a. A real-component example of such component cracking is shown in Figure II-5b. A photo elastic image of the strain fields induced by split sleeve cold working is shown in Figure II-5c.

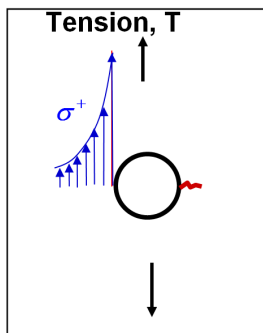


Figure II-5a. A schematic of the tensile stress enhancement they are a whole under tensile loading and a position of a fatigue crack in this geometry. environment. (Proceedings of the 2007 Residual Stress Summit.)



Figure II-5b. A picture of fatigue cracks emanating from hole stress concentrations in a rotor and oriented transverse to the under operation tensile loading direction. (Internet)

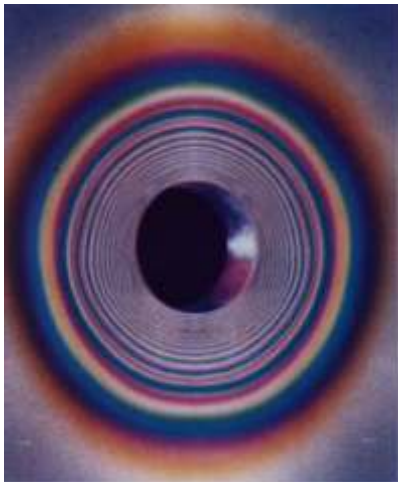


Figure II-5c. Photo elastic surface evidence for the compressive strain fields introduced around a hole that has been subjected to split sleeve cold working. (Proceedings of the 2007 Residual Stress Summit.)